Effect of shrinkage on slant shear and flexure bond strength of cement based micro-concrete for durable concrete repair

Dipti Ranjan Nayak[1] · Rashmi R. Pattnaik[2] · Bikash Ch. Panda[1]

Abstract

The micro-concrete repair failure is a subject of concern since the information about the bond strength is not available in literature. The available data on bond strength differs based on the type of test procedure used in various studies, there is no universally accepted test protocol available for determining the bonding strength of cement-based micro-concrete. In the present work, two test methodologies investigated for measuring the bonding strength of micro-concretes. The slant shear and the three-point flexure tests were conducted similar to ASTM C882and ASTM C348 test procedure, respectively. Mechanical properties such as compressive strength and flexure, as well as durability property, such as drying shrinkage of the micro-concretes were determined to support the evaluation of bonding strength. Further, the specimens were analyzed using finite element analysis (FEA) to find reasons behind the failure patterns. It was observed that the compressive strength of the micro-concrete does not influence any kind of bonding strength calculations. The stress concentration and displacement at the joint near the low bond strength elements were found to be disproportionately high as indicated by FEA, causing the specimens to fail sooner than those with high bond strength elements at the interface.

Keywords Micro-concrete · Concrete repair · Drying shrinkage · Bond strength · Repair materials

1 Introduction

Micro-concrete is a type of concrete with tiny aggregates and of mostly used for shallow concrete repair work. To make it flowable micro-concrete, only clean water was added on site according to the manufacturer's specifications. It is difficult to find an appropriate micro-concrete for a concrete repair due to non-availability of micro-concrete having uniform strength. Concrete repairs are usually carried out to extend the life of an existing structure and restore the structure's load-bearing capacity by enhancing strength of the members. Repairs are typically performed at the joints or in strained areas of the concrete structure which are subjected to various stresses [24]. Aside from mechanical strength, the bonding strength between the repair material and the substrate concrete is a critical property to evaluate. The bonding strength of micro-concrete is a critical parameter to the success of concrete repair [21–23]. The tested bond strength is largely dependent on the procedures employed in the test. Due to the complexities of each test procedure, there is no consensus on which one to use. The slant shear test has become popular due to its simplicity and has been adopted by various international specifications for testing the bond strength of repair materials. Researchers at the University of Arizona proposed the slant shear test approach [18] which is also included in the BS EN 12615 and ASTM C882 [6] provisions. The test was carried out on a composite of repair materials and substrate concrete, which was linked on a slant elliptical plane at a 60° angle to the horizontal cross sectional plane. A compressive strength test equipment was then used to load the composite cylinder. The shear force on the elliptical slant area at the failure load is used to calculate the bond strength. Previous study has found that the rupture does not occur on the slant area for all types of repair materials. The failure depends on the strength under compression of the substrate concrete and the repair materials [1, 20, 27, 28, 30]. The slant shear bond strength is observed to increase as the compressive strength of the repair materials increases. In addition, the shape of the composite specimen plays a role. Prism specimens represent more reliable values of slant shear

✉ Dipti Ranjan Nayak
diptiranjan.1979@gmail.com

1 Department of Civil Engineering, Indira Gandhi Institute of Technology, Dhenkanal, Odisha, India

2 Department of ASCEE, CAET, Orissa University of Agriculture and Technology, Bhubaneswar, India

strength than cylindrical specimens, according to Diab et al. [11].

The tensile test process of substrate and repair materials is used to determine the bond strength of the repair materials under tensile stress, as most failures are caused by tension in the concrete. However, even a minor misalignment in this test process can result in significant scatter in the data. A proper tension test is also difficult to perform as well as time-consuming. According to Courard et al. [9], a 2° misalignment reduces pull-off bond strength by 7–9%, and a 4° misalignment reduces pull-off bond strength by 13–16%.

Momayez et al. [19] has reported a comparison of four test methods for evaluating bond strength, such as pull-off, slant shear, splitting prism, and a new Bi-Surface shear. The test results were different in these four test methods, and the magnitude of bond strengths were higher, even up to eight times larger, from one test method to another test method. As a result, it was advised that the bond strength test technique should be chosen based on the stress of the substrate concrete of the structure. Piancastelli et al. and Wall and Shrive [25, 30] found that the finite element model (FEM) can imitate the behavior of bonding materials due to mismatch of modulus of elasticity in their investigation on slant shear bonding strength between new and existing concrete using experimental and finite element methods. The mesh's bond line elements were segregated from the rest of the mesh. Different moduli of elasticity of the elements were used to simulate bond weakening. The modulus of elasticity of the bonding materials was determined to be desired when compared to the nearby concrete. The bonding strength is significantly reduced when the bonding layer is thicker.

Concrete repair is typically carried out at connections, and strain is created in the concrete repair due to bending of the concrete structure caused by transverse loading or changes in the environment. The flexural bond strengths of micro-concretes were examined in this work utilizing a modified ASTM C348 [5] flexural strength test technique. The substrate concrete cylinders were split in half and patched with six different micro-concretes to create composite cylinders in this test method. To evaluate the early and later ages of repair, the composite actions of substrate concrete and micro-concrete were investigated after 3, 14, and 28 days of patching.

The flexure bond strength and the failure patterns were investigated using a high precision universal testing machine and finite element analysis.

2 Research significance

The bond strength between the substrate concrete and the cement-based micro-concrete is an important attribute to investigate during the restoration process. The quality of the micro-concrete bonding determines the effectiveness of concrete infrastructure repair and restoration. Due to misunderstandings in concrete repair, there are many failures and continuous "repair of repairs" [29]. Since there is no standard test technique for evaluating the bond strength of cement-based micro-concrete, achieving long-lasting concrete repair is found to be difficult. The available data on the failure of repairs are scarce owing to bonding. This article investigates the experimental test procedure of flexure bonding along with slant shear, mechanical strength, and the resilience properties of the materials Furthermore the failure pattern has been studied through finite element model to pick a suitable micro-concrete for a durable concrete repair due to bending.

3 Experimental method

3.1 Materials used for experiments

From the regularly used micro-concrete for low depth concrete repair, six distinct cementitious micro-concretes, a to F, were chosen. The amount of water blended in such a way that the flow on the flow table remains constant at 120 mm. Cement containing mineral and chemical admixtures, as well as fine particles, are examples of well-known forms.

> A, B, and C = Engineered micro-concrete with OPC, Ordinary Portland Cement of grade 53 (28 days compressive strength is 53 MPa) conformed to IS 12269 [14], Portland Pozzolana Cement (PPC) Fly ash based as per IS 1489 (Part 1) [15] and Portland Slag Cement (PSC) as per IS:455 [13], respectively, with small aggregate, cement to the aggregate ratio of 1:1 and superplasticizer, powdered Poly-carboxylate ether were used.
> D, E, and F = Ready mix micro-concrete of OPC with fly ash, Silica fume, and smaller aggregate in different proportion as noticed through SEM and EDS systems, and also observed through sieve analysis

Besides micro-concretes, OPC grade 53 along with smaller aggregate of maximum size of 4.75 mm was used for preparing substrate concretes. The mix proportion and grading of the substrate concrete is shown in the Table 1.

The substrate concretes for the slant shear bond strength and the composite specimen for three-point flexure test were made from the same mix proportion.

Table 1 Mix proportion and grading of aggregates for substrate concrete

(a) Mix proportion		
Cement	378	kg/m^3
Water	178	kg/m^3
Small aggregate	851	kg/m^3

(b) Gradation of the small aggregates		
Passing	Retained on	Mass, %
4.75 mm	2.36 mm	10
2.36 mm	1.18 mm	25
1.18 mm	600 μm	25
600 μm	300 μm	25
300 μm	150 μm	15

3.2 Specimen preparation and experiments

3.2.1 Morphological and elemental analysis

The morphological and elemental analysis of micro-concrete was carried out by using Scanning Electron Microscope and Energy Dispersive Spectroscopy (SEM–EDS) (Zeiss-EVO18) in order to make the sample's conductivity, powdered samples were evenly dusted over a carbon tape, followed by a conductive gold sputtering coating. The presence of multi-phase particles is shown by the changing the contrast from brighter to darker in the backscattered electron (BSE) images. Lighter atoms with a lower atomic number produce dark contrast, while heavier elements with a higher atomic number produce a brighter contrast. The existence of the particular element at the micro-constituent level is confirmed by using an Energy Dispersive Spectrometer (EDS) attached to the SEM as demonstrated in figure.

3.2.2 Sieve analysis

A series of sieves with size of 2.36 mm, 1.18 mm, 600, 300, 150, 75, 45, and 25 micron were used to sieve 400 g of each micro-concrete as per IS:2386 (part-I). A sieving duration of 20 min was set in the sieve shaker for each sample to allow sufficient time for the material to pass through the set of sieves. The weight retained, percentage of passing, and cumulative percentage of passing were determined after end of sieving operation. To grade the micro-concrete from coarser to finer, the cumulative percentage of micro- concrete passing through a 150- micron screen was taken into consideration.

3.2.3 Compressive strength

In both micro concrete and substrate concrete samples, smaller particles less than 4.75 mm were used. As per the ASTM C109 [4] test technique, 50 mm (2 in) cube moulds were employed. The cubes formed with the micro concretes were evaluated after 3, 14, and 28 days from the day they were cast. While the substrate concrete was evaluated after 38, 49, and 63 days, respectively, the micro-concretes bonded with the substrate concrete were tested after 3, 14, and 28 days.

3.2.4 Free shrinkage

The ASTM C 157 [2] test protocol was used to record the free dry shrinkages of the substrate concrete and micro-concretes using a length comparator. This testing process determined free shrinkage of materials with dimensions of 25 mm×25 mm×285 mm, with a gauge length of 250 mm. After 7 days of curing in a damp environment, the materials were dried in an oven at 50 °C for 6 h.

3.2.5 Flexure strength with and without bonding

The flexural strength was determined using a circular cross-section keeping a point load in the center of the beam as shown in Fig. 1. The flexure strength of a material is its greatest bending strength under pure bending. The center and bottom portions of the specimen are subjected to the largest bending stress when loaded. Depending on the binding strength between the micro concrete and the substrate concrete, the composite material's flexural strength will be high or low. The flexural strength was calculated using the following Eq. (1) for the test setup as displayed in Fig. 1.

$$\sigma = \frac{8WL}{\pi \rho^3} \tag{1}$$
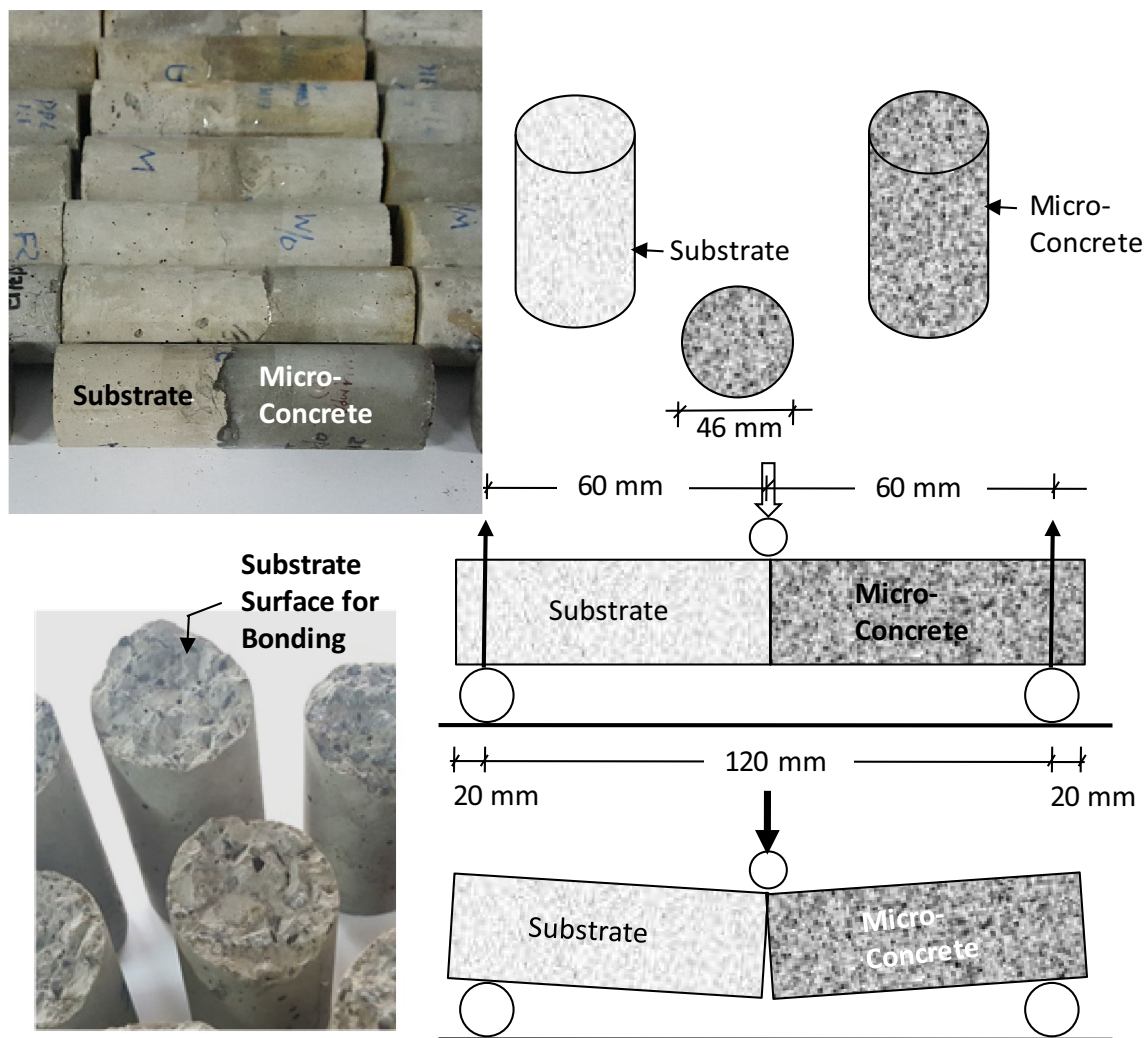
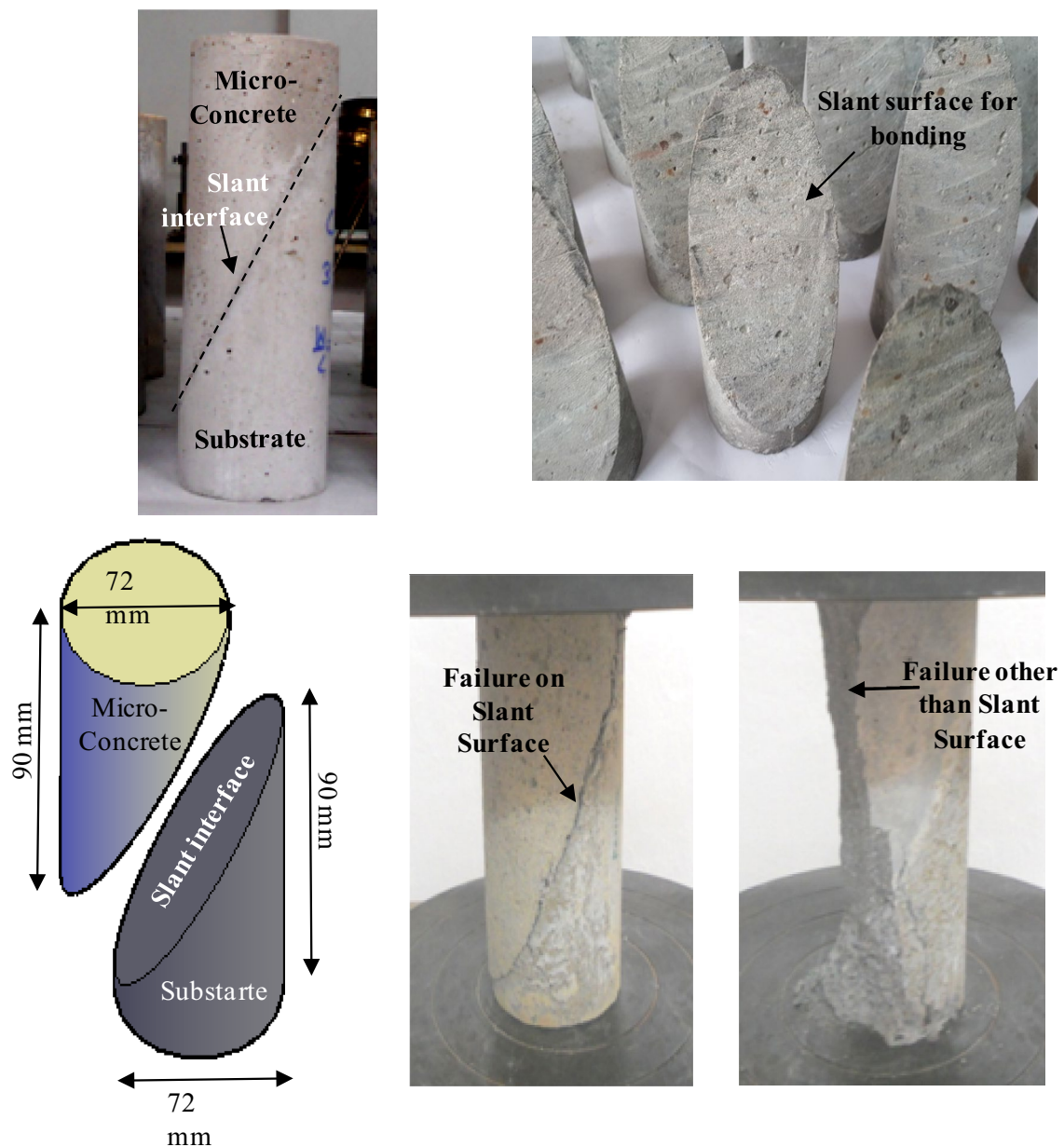**Fig. 1** Composite specimen preparations and flexure loading for bond strength

where σ = Flexural Strength of the material; W = Point load on the top at failure; L = Span between the two supports, 120 mm apart; ρ = diameter of the cylinder which is 46 mm.

Cylindrical molds of 46 mm diameter × 160 mm height were used to test the flexure strength of substrate concrete and micro-concrete cylinders. The supports and loading conditions on the specimens were tested according to ASTM C348 [5]. To retain the vertical position of the composite materials, a cylindrical specimen was preferred over a prismatic specimen. On the 28th day after its casting, the substrate concrete was examined. Following the testing, the two portions of approximately 80 mm length were cemented with the micro-concretes A to F. for the composite material's flexural bonding strength Because the surface was already uneven, unlike the slant shear test illustrated in Figs. 1 and 2, the fragmented faces of the substrate concrete were produced with saturated surface dry state and bonded without scrubbing. After 3, 14, and 28 days of bonding, the composite

material was subjected to the same flexural strength test procedure, involving the application of a point load at the junction between substrate concrete and micro-concrete until failure occurred [7]. For the flexure testing, a 5 kN UTM was used to record the load and displacements. For further study on the flexure test findings, the deformation curves and breakdown patterns of the composite material were also observed. The composite specimens' results were compared to finite element analysis of composite finite element models, and they were found to be similar.

3.2.6 Slant shear test

The micro-concretes were laid the elliptical slant surface of the substrate concrete, inclined at an angle of 60° with the horizontal axis in the slant shear test process, as illustrated in Fig. 2, in order to form a 72 mm × 180 mm cylinder shape composite materials. Before the micro concretes

Fig. 2 Composite specimen preparations, slant shear loading and failure for bond strength

were installed over the surface, the substrate concrete's elliptical slant planes were made even by wire scrubbing, cleaning, and washing. After roughening the slant sections, they were allowed to cure air for 7 days before bonding the micro-concretes. The tests were carried out after 3, 14, and 28 days of casting to determine the strength under slant shear conditions. The slant shear strengths were calculated by the maximum compressive load acted on the cylindrical specimen to break the composite material, [*Load at failure*]/[*slant elliptical area*]. The slant shear strengths reported were the mean of 3 composite cylinders for every micro-concrete sample at each period.

3.2.7 Finite element model (FEM)

The following objectives of the finite element analysis were focused on the three-dimensional stress system of the cylindrical composite specimen and the finite element models are made and analyzed using SAP2000 FEM software.

i. Major principal stress distribution at the bottom of the cylindrical specimen due to different moduli of elasticity of micro-concrete and substrate concrete with poor and strong bond strength element at the interface

ii. Deformation of the composite specimen due to poor and strong bond strength element at the interface

Figure 3 depicts the finite element model used to calculate the flexural bond strength. For the flexure test, eight and six nodded solid pieces were employed to represent the cylindrical composite specimen. 3136 solid components were used to simulate the substrate concrete. To capture the stress distribution at the tension area, the sizes were made coarser to finer throughout the length of the cylinder and from the middle of the section to the outer of the section. Solid elements ranged in size from 5 mm×5 mm×5 mm at the ends to 1 m×1 mm×1 mm at the interface were considered. Similarly, 3332 solid elements were used to model the micro-concrete. Where as, out of 3332 solid elements, 195 elements near by the interface were modeled from 5 mm×5 mm×1 mm to 1 mm×1 mm × 1 mm towards circumference. The poor and strong bonds of the interface were simulated by changing the modulus of elasticity of those interface elements [30]. The modulus of elasticity of the substrate and micro-concrete were calculated based on the compressive strength as calculated in the experiments using the [16], Cl.6.2.3.1 and following Eq. (2) as follows.

$$E = 5000 \times \sqrt{f_c} \qquad (2)$$

where E = Short term static modulus of elasticity and f_c = Compressive strength of the materials (N/mm^2).

Modulus of elasticity (E) for M18 substrate concrete was calculated to be about 21 GPa. The two different E values for the micro-concretes were calculated as 32 GPa and 16 GPa when represent two different compressive strengths of the micro-concretes. Two different moduli of elasticity were used for the interface elements, 1.0 GPa for poor bondage and 10 GPa for high bondage to investigate two different bond strengths of the micro-concrete corresponding to the flexible and stiffer bond strength of the materials, respectively [30]. The modulus of elasticity of low and high bond strength at the interface for low compressive strength micro-concrete were 6.25% and 62.5%, respectively. Similarly, for high compressive strength micro concrete, the modulus of elasticity at the interfaces were 3.125% and 31.25% of that of the micro concrete. Poisson's ratio of concrete varies from 0.15 to 0.25. For this test, the possion's ratio of 0.17 was selected for all solid elements. Thus the assumptions were made similar to the experimental investigation; although a small amount of surface roughness exists. However, even with the limitation, finite element analysis is still capable of
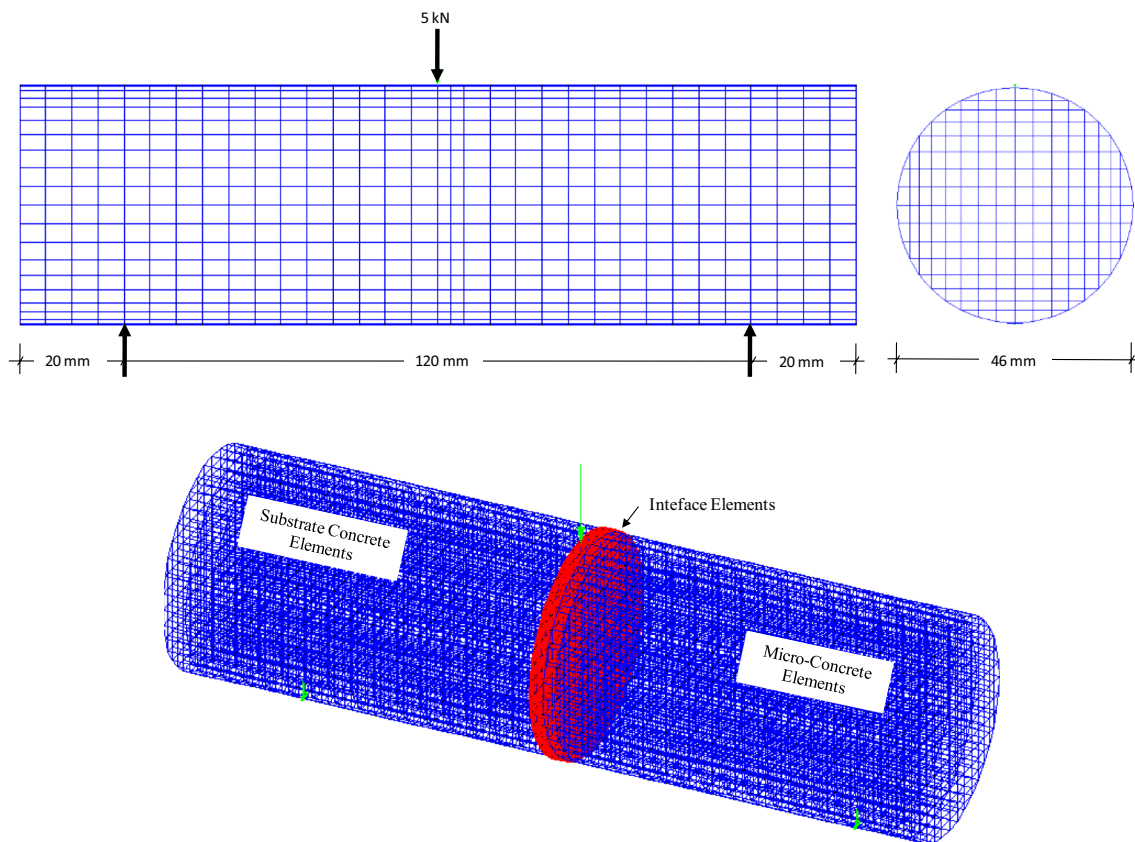

Fig. 3 Finite element model of composite specimen for flexure test

providing useful information. The followings are the four different conditions of the FEM specimens. The moduli of elasticity for the Substrate, Interface and Micro-Concrete of the FEM specimens were-

FEM A = 21, 1, 16 GPa;

FEM B = 21, 1, 32 GPa;

FEM C = 21, 10, 16 GPa; and

FEM D = 21, 10, 32 GPa, respectively.

The testing was simulated in the finite element model by applying a 5kNload at the top surface of the interface elements of the composite cylinder. The cylindrical specimen was simply supported at 20 mm from each end of the cylinder as shown in Fig. 3.

4 Results and discussions

4.1 Major principal stress in the finite element analysis (FEA)

Due to the central load at the top, as shown in Fig. 3, the major principal stress was maximum at the bottom middle portion of all four composite specimens, FEM-A to D. Figure 4 shows the major principal stress distribution of the composite specimens. To capture the maximum bending stress, the color code of the stress distribution was made in the range of 0–20 MPa. When a single material modulus of elasticity value was recorded throughout the specimen, the maximum stress was observed at the bottom centre point. Due to a mismatch in the moduli of elasticity of the substrate, interface, and micro-concrete, the maximum stress was shifted to the material's superior modulus of elasticity. The maximum stress in FEM-A and C moved towards the substrate, whereas FEM-B and D moved towards the micro-concrete. As demonstrated in Fig. 4 FEM-A to D, the stress concentration at the bottom centre region was varied. Figure 4 depicts the front aspect of the composite cylinders'

major principle stress distribution with low and high bond strength parts. The stress concentration near the middle of the bottom face of the prism is greater than the high strength of the material elements for poor bond strength or interface elements. The stress variation was within 4% from maximum to minimum due to a change in only one variable, the modulus of elasticity; yet, the stress variation was effective in visualizing the actual composite specimen in the experimental test with respect to the modulus of elasticity. For the cases of FEM-C and D of the composite model, it was noticed that the stress concentration at the bottom interface decreased for the superior strength components at the interface, as shown in Fig. 4. It indicates that if the interface bond strength is strong, the composite cylinder will have high flexural strength, and the composite specimen with low bond strength will fail sooner than the high bond strength material at the interface.

4.2 Maximum displacement at bottom

It was observed in the FEA that the displacements were higher with low-strength elements between the substrate and repair materials. The displacement was maximum in the case of FEM-A model. The displacements were reduced with higher strength elements between the micro concrete and the substrate. The displacement was minimum in the case of the composite prism FEM-D model. More movements were observed in the FEM with low strength material at the interface which was also observed in the load–deflection curves of the experimental results even with a different type of cement content as noticed in the EDS results.
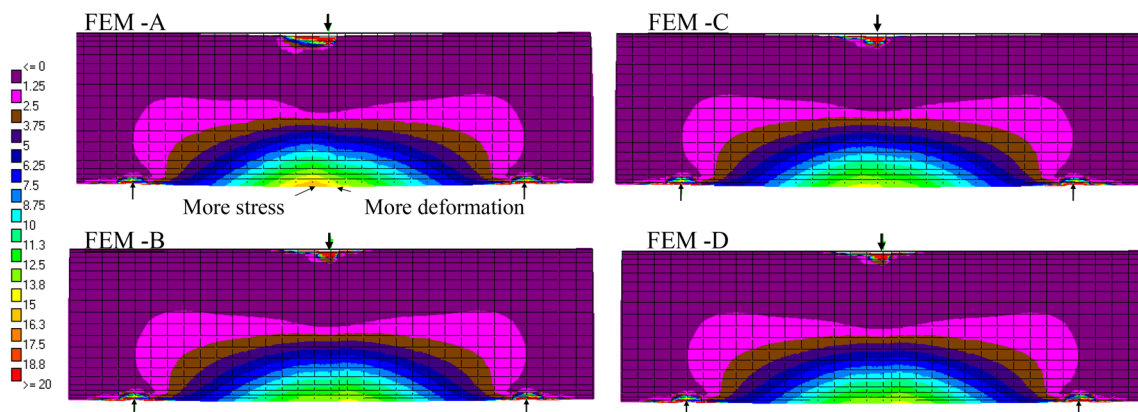

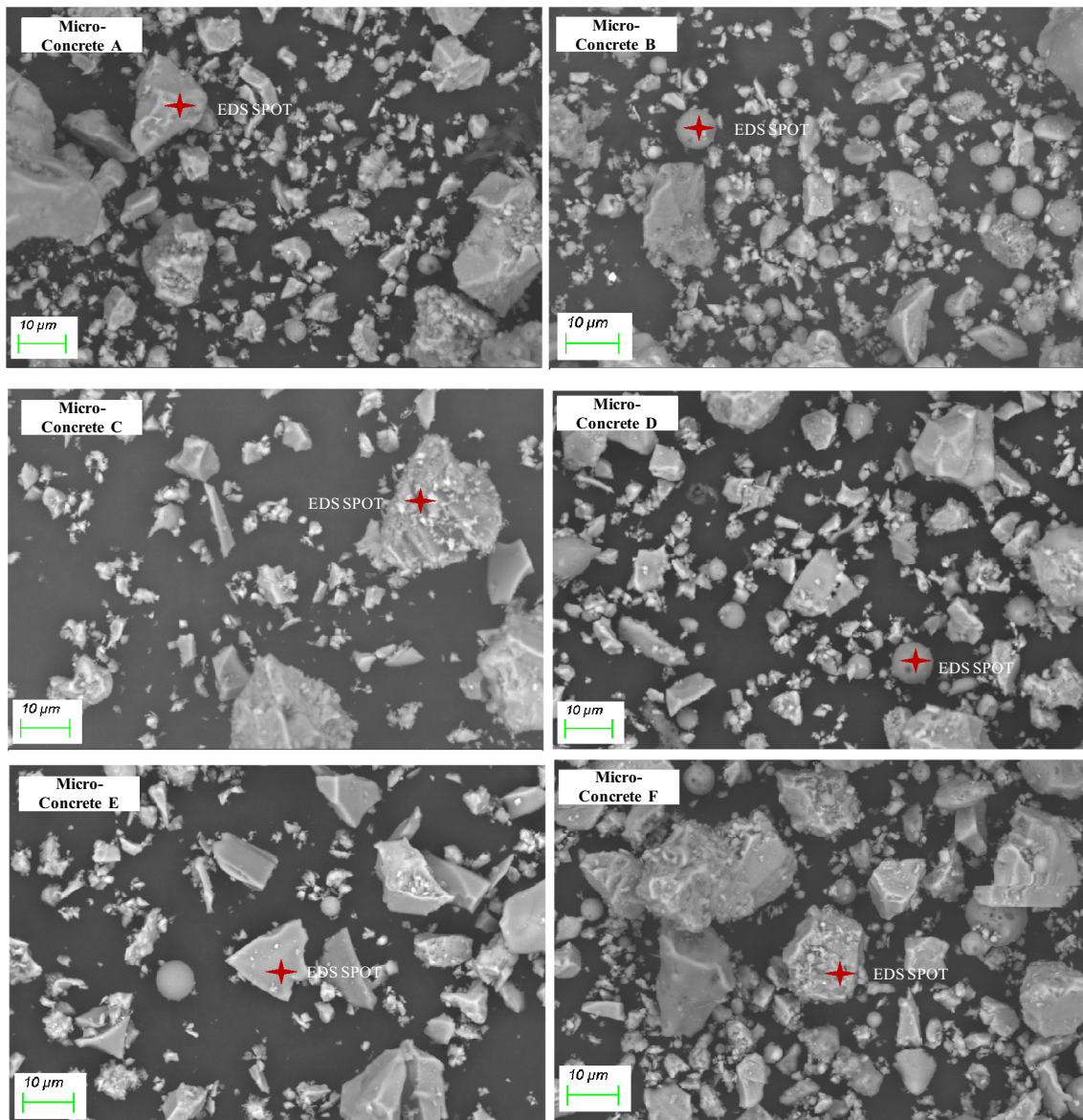**Fig. 4** Major principal stress distribution in the composite specimen

Fig. 5 SEM images of the micro-concrete A to F

4.3 Scanning electron microscope (SEM) images and energy dispersive spectroscopy (EDS) results

Figure 5 presents the SEM images of the micro-concretes A to F. Particles as observed on the figures are varied, very large particles as well as many smaller ones. Moreover, the size and shapes of the particles vary from spherical to irregular shapes. To characterize the micro-concrete, six different spots on each micro concrete were selected and analyzed in terms of chemical composition. Figure 5 shows one of the six spots and its result in Fig. 6. In the EDS analysis confirmed that each particle varies in its elemental composition. The spherical particle is rich in oxides of aluminum and silicon and little amount of oxides of iron and potassium, as observed in micro concrete B and D. The irregular shaped particle has oxides of Ca, Al, Si, Mg, and little amount of Fe as in micro concretes A, E, and F. The particle in the micro-concrete C contains both sulphide and oxide of calcium. The following elements were observed in the micro-concrete on six different spots of the micro-concrete surface.

A = Ca, Si, Fe and Al;
B = Si, Ca, S, O, Al, Fe and Mg;
C = Si, Ca, S, Al, Mg, and C;
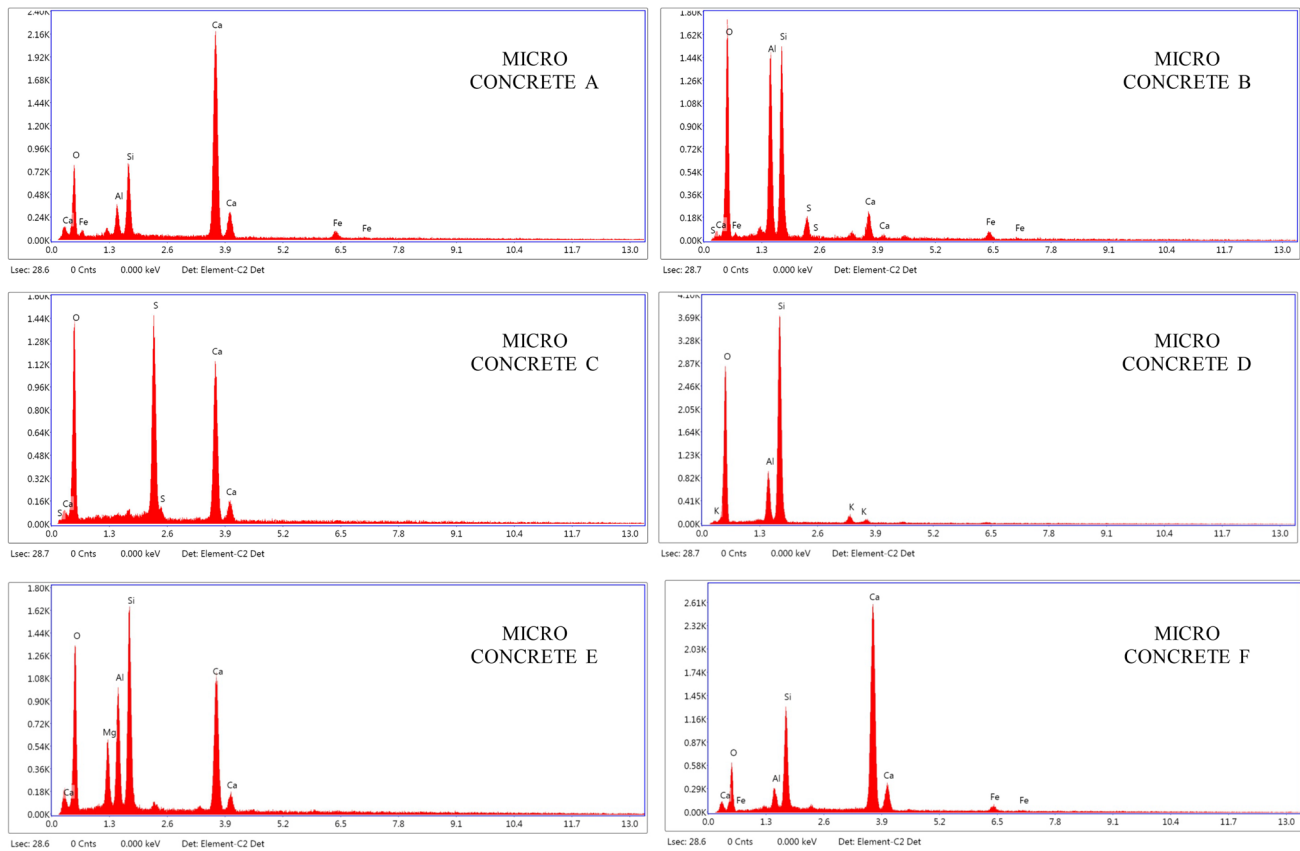D = Ca, Si, O, Al, K, Fe, and Mg;

Fig. 6 EDS SPOT characterization of the micro-concretes

Table 2 Sieve analysis of the micro-concretes A to F

Sieve size in mm	Repair materials (Cummulative % passing)					
	A	B	C	D	E	F
2.36	100	100	100	99.9	100	99.6
1.18	85	85	85	84.7	88.8	86
0.6	70	70	70	71.5	70.4	70.8
0.3	55	55	55	57.5	52.8	52.6
0.15	48.25	48.63	33	47.5	39.2	43
0.075	10.75	11.23	4.4	11.9	8.8	31
0.045	1.25	0.94	1.2	1.5	2	8.2
0.025	0.25	0.2	0.2	0.3	0.8	3
Pan	0	0	0	0	0	0

E = Ca, Si, Na, Al, O, Fe, Mg, and K;
F = Ca, Si, O, Al, Fe, and Mg.

4.4 Grading of micro-concretes

The cumulative percentage of aggregate passing through the sieves from 2.36 mm to 25-micron sieve of six different micro-concrete from A to F is shown in Table 2. It can be observed that almost all the micro-concretes were below 2.36 mm particle size. The cumulative percentage of passing through150-micron sieve in the micro-concrete C was minimum (33%) and the micro-concrete B was the maximum (48.63%). Therefore, the sequence of coarser to finer micro-concrete was C, E, F, D, A, and B.

4.5 Strength under compression

The strength under compression is not an essential property in many repair usages. However, the compressive strength has been considered as the single most property for the

Table 3 Compressive strength of the micro-concretes

Micro-Concrete	Compressive strength in MPa		
	3 days	14 days	28 days
A	35.74	47.28	56.76
B	31.63	36.37	45.27
C	35.69	37.35	41.71
D	39.96	43.02	55.93
E	39.08	46.53	65.28
F	17.96	25.01	42.39

selection of repair material in case a concrete repair [26]. The compressive strength of the micro concretes at 3, 14, and 28 days are presented in Table 3.

The results of each period at 3, 14 and 28 days are the mean of 3 specimens. It was observed that the micro-concrete E had maximum compressive strength of 65.28 MPa at 28 days and micro-concrete C had a minimum 41.71 MPa under the same curing condition. It was also observed that the strength gained at 3, 14, and 28 days were different for different micro-concrete. The sequences of micro-concretes exhibiting highest to lowest compressive strength are D, E, A, C, B and F, at 3 days, A, E, D, C, B, and F, at 14 days and E, A, D, B, F, and C at 28 days.

4.6 Slant shear strength

Table 4 shows the average of three specimens per test of slant shear bond strength of the micro-concretes at 3, 14, and 28 days from the days of the casting of micro-concretes on the substrate concrete. The failures of the composite cylinders were noted down whether the failure occurred on slant surface or not. The slant shear bond strength of repair material A was the highest (18.56 MPa) at 28 days and that of repair material C was the lowest (7.3 MPa). If two specimens out of three were failed on slant surface, then recorded "Yes" or else "No" as shown in Table 4. It was observed that none of the ready mix micro concretes, D, E and F failed on the slant surface at 28 days. The sequence from weaker to

the stronger bond strength of the materials as measured at 3 days, 14 days and 28 days were D, B, A, E, F, and C, A, D, F, B, E, and C, A, D, E, F, B, and C, respectively. The sequences in all three ages were not the same. However, the micro-concrete C prepared with cement PSC showed the lowest strength in all three ages.

In Tables 3 and 4, it was observed that at early ages of 3 and 14 days the micro-concrete D and A gained maximum compressive strength, respectively. The slant shear bond strength of those micro-concretes was found to be highest at the ages of 3 and 14 days. Slant shear bond strength increases as the compressive strength of higher strength micro-concrete mixtures increases. Júlio et al. [17] have reported similar results to that observed in the present study. At 28 days, however, the tendency was not the same. The trend was similarly absent in the examination of flexural bond strength. As a result, the flexural bond strength of the micro-concrete was not affected by its compressive strength. The bond strength of the composite cylinder owing to flexure testing did not get affected by the compressive strength of the micro-concrete.

4.7 Free shrinkage of the materials

The free drying shrinkage values of the micro-concretes are shown in Fig. 7. The readings on the graph reflect the average of three specimens' results. The greater and lower free shrinkage values achieved at 3 days and 28 days were not in the same order. The sequence from lowest to highest free shrinkage at 3 days was B, C, D, A, F and E; whereas, the sequence at 28 days B. D, A, C, F, and E for all micro-concretes under similar environmental condition.

At present there is no permissible free shrinkage limit. However, ASTM C 928 [3] provides the limit for the packed cementitious concrete repair material as 0.15%. Decter and Keeley [10] suggested that the free shrinkage limit of 500 μs (0.05%) at 28 days or 300 μs (0.03%) at 3 days is the safe limit for a durable concrete repair. Emmons et al. [12] mentioned that any repair material at 28 days' shrinkage less than 500 μs (0.05%) regarded as low shrinkage material,

Table 4 Slant shear strength of the micro-concrete A to F

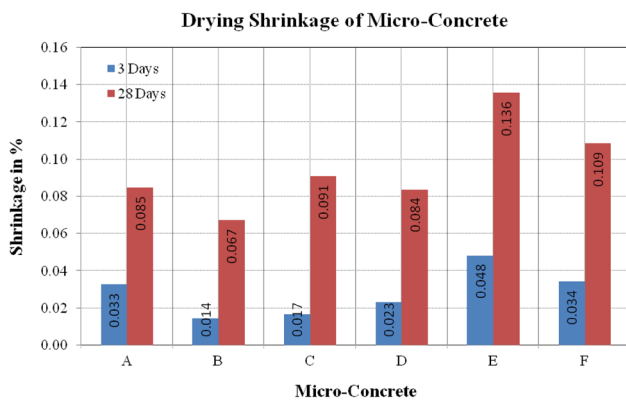| Repair materials	3-days		14-days		28-days	
	Slant shear strength in MPa	Failed on slant surface	Slant shear strength in MPa	Failed on slant surface	Slant shear strength in MPa	Failed on slant surface
A	7.62	Yes	13.57	Yes	18.56	Yes
B	8.21	Yes	10.82	Yes	11.53	Yes
C	5.53	Yes	5.94	Yes	7.3	Yes
D	9.64	Yes	11.34	No	15.89	No
E	7.07	Yes	10.21	No	14.82	No
F	6.71	Yes	11.27	Yes	11.59	No

Fig. 7 Drying shrinkage of the micro-concretes at 3 and 28 days

500 μs (0.05%) to 1000 μs (0.1%) as moderate and more than 1000 μs (0.1%) as high shrinkage material. It was noticed that all repair materials in this investigation showed free shrinkage of more than 500 μs (0.05%) after 28 days because of the temperature conditioning which is the moderate shrinkage. The free shrinkage of the micro-concrete B was the lowest at 670 μs (0.067%) at 28 days and that of the repair material E was the highest at 1360 μs (0.136%).

Among the six micro-concretes tested, the micro-concrete E exhibited the maximum compressive strength after 28 days. According to a prior study, the stronger the compressive strength, the higher the slant shear bond strength. However, in the slant shear bond strength, the bond strength of micro-concrete E was not the strongest. This may be attributed to the fact that it has the highest drying shrinkage value of all the micro-concretes, at 1360 s (0.136%). This suggests that the drying shrinkage of the micro-concrete affects the material's bonding strength. The micro-concretes D and A showed a lower drying shrinkage value of 0.084% which performed better results in the slant shear and flexural bond strength of the micro-concretes.
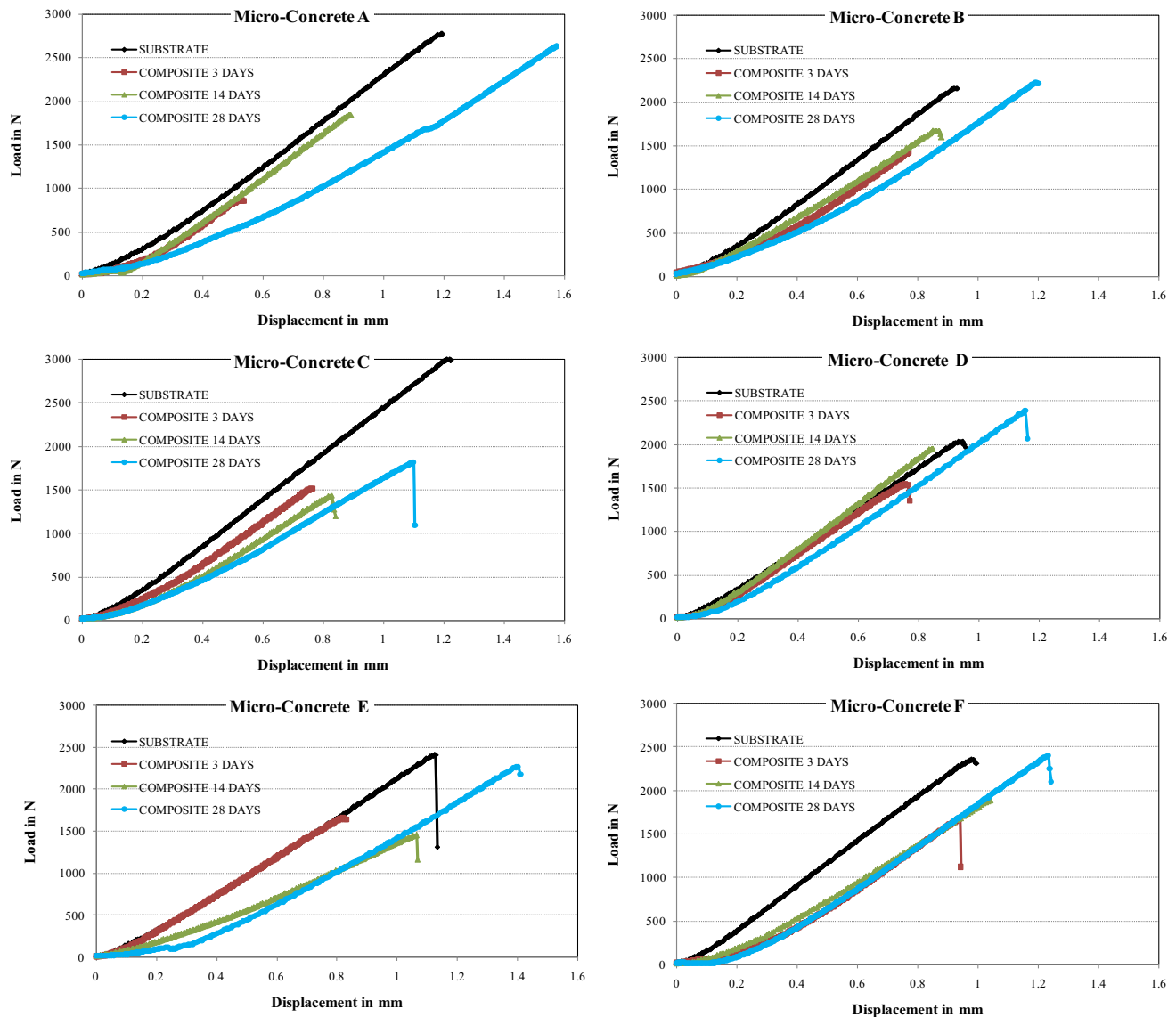
4.8 Flexural bond strength

The flexure strength of substrate concrete and six different types of micro-concrete composite materials after 3, 14, and 28 days are shown in Table 5 in addition, the flexure strength of the composite cylinder was also estimated in comparison to the comparable flexural strength of the substrate and micro-concrete at that age (Table 5). All of the composite cylinders had lower flexural strength as compared to that of the substrate concrete cylinder after 3 and 14 days. On the 28th day, the micro-concrete B, D, and F demonstrated stronger flexural strength than the substrate concrete's corresponding flexure strength. Micro-concrete D displayed the maximum flexure bonding strength at 28 days in comparison with all other micro-concretes. Micro-concrete C showed the minimum flexure bonding strength which is similar to the slant shear bond strength evaluation result of the micro-concretes.

Table 5 also illustrates the percentage rise and reduction in composite cylinder flexure strength in relation to substrate concrete and micro-concrete flexural strength. At 28 days, all composite specimens of ready mix micro concrete D, E, and F demonstrated higher flexure strength than that of the micro-concrete. At 3, 14, and 28 days, the micro-concrete F flexural strength of the composite cylinder was higher than the comparable flexural strength of the micro-concrete. This increase in strength implies that the binding strength between the micro-concrete and the substrate has improved.

Figure 8 shows the combined load-deformation curves of the UTM, which were used to further investigate the flexural bond strength. At 3, 14, and 28 days, the four curves in each micro-concrete, the substrate concrete, and the composite cylinders were superimposed. The micro-concrete D had stiffer composite cylinder curves for 3, 14, and 28 days, which were nearer to the substrate concrete, having the maximum flexural bond strength of all the micro-concrete. Except for micro-concrete D, all other composite cylinders of micro-concrete showed distinguishable movement at the

Table 5 Flexure strength of composite cylinders

Micro-con-crete	3 days			14 days			28 days		
	Flexure bond in MPa	Increase of flexure strength from substrate (%)	Increase of flexure strength from micro con-crete (%)	Flexure bond in MPa	Increase of flexure strength from substrate (%)	Increase of flexure strength from micro con-crete (%)	Flexure bond in MPa	Increase of flexure strength from substrate (%)	Increase of flexure strength from micro concrete (%)
A	3.41	− 51	− 99	5.62	− 22	− 49	7.07	− 15	− 27
B	4.59	− 42	− 18	5.56	− 14	− 1	5.57	11	− 12
C	4.82	− 47	− 72	4.31	− 38	− 105	5.34	− 23	− 71
D	4.60	− 29	− 2	5.86	− 15	10	7.13	17	8
E	5.35	− 26	12	4.50	− 40	− 28	6.49	− 25	9
F	4.78	− 32	15	5.23	− 28	6	6.84	11	12

Fig. 8 Load deflection curves of the substrate and composite specimen

interface, resulting in a flatter slope than the substrate concrete. The micro-concrete F, on the other hand, had the highest flexure strength of the composite cylinder as compared to that of the substrate concrete.

4.9 Comparison of bond strength due to slant shear and the three-point flexure test

One of the most critical aspects determining the reliability and durability of concrete repairs is bond strength. The strength of the bond between the micro-concrete and the substrate concrete is controlled by the strength of the interfacial zone. Slant shear and flexure test procedures were simple to prepare as well as analyses. The bond strength is typically determined by the stress in the structure where the

micro-concrete will be installed. Shear stress is the most common cause of bond failure in most applications. The bond strength measured during bending is believed to be lower than the bond strength measured under shear stress. In the present study the micro-concrete bond strength calculated using slant shear bond strength was found to be 1.5–3 times higher than the flexural bond strength for the identical micro-concrete in this study. In both situations, the bond strength values of the micro-concrete trended in the same direction. However, unlike the slant shear bond strength test, the flexural bond strength test may be used to examine the percentage of increase in flexure strength for composite specimens against the substrate and micro-concrete material employed on the study.

5 Conclusions

Micro concretes are small aggregate ready-mix concretes made with OPC, PPC, and PSC cement. These concretes are mostly utilized for shallow depth concrete restoration in areas with inaccessible and thick reinforcements, which are difficult to pour for repair with regular concrete. The following references are drawn from experimental tests and FEA on bond strength of micro-concrete:

- The bond strength of micro-concrete varies depending on the test methods employed. The magnitude of the slant shear test method was greater than the flexure test method, while evaluating bond strength.
- The bond strength of the micro-concretes assessed by two different test methods did not follow the same patterns. As a result, the bond strength test technique must be chosen based on the type of stress like compressive or tensile stress, the location, where the micro-concrete will be used.
- The advantage of evaluating flexure bond strength while choosing micro-concrete is that the flexural strength of the composite cylinder can be computed ahead of time and it will indicate the differences of flexural strength the composite material, the substrate and micro-concrete.
- The deformation at the interface can be detected using load deflection curves similar to those used in FEA to determine the stiffness of the micro-concrete interface.
- The cylindrical specimen can be made by cutting a cylindrical core from the actual construction using a core-cutter and patching it with micro-concrete to the desired length for analyzing the bond strength as well as the micro-concrete compatibility with the actual substrate concrete.

In order to evaluate the bond strength of micro-concrete exposed to bending, the flexure bond test process has the potential to become an effective test method for samples prepared in the laboratory and samples extracted in a core cutter on site. Future research may be focused on the bonding agent utilized on the interface before inserting the micro-concrete to assess the bond strength increase caused by bending.

Declarations

Conflict of interest The authors declare that they have no conflict of interest.

References

1. Abu-Tair AI, Rigden SR, Burley E (1996) Testing the bond between repair materials and concrete substrate. ACI Mater J 93(6):553–558
2. ASTM C 157 (2014) Standard test method for length change of hardened hydraulic cement mortar and concrete. ASTM International, West Conshohocken
3. ASTM C 928 (2014) Standard specification for packaged, dry, rapid-hardening cementitious materials for concrete repairs. ASTM International, West Conshohocken
4. ASTM C109 (2002) Standard test method for compressive strength of hydraulic cement mortars, vol 04. American Society for Testing and Materials, Philadelphia, pp 1–6
5. ASTM C348 (2002) Flexural strength of hydraulic-cement mortars, vol 04. American Society for Testing and Material, Philadelphia, pp 1–6
6. ASTM C882 (2005) Standard test method for bond strength of epoxy-resin systems used with concrete by slant shear. American Society for Testing and Materials, Philadelphia, pp 1–3
7. Bhoi KC, Pattnaik RR (2018) Investigation into low density fly ash aggregate in micro-concrete for lightweight concrete repair. J Build Pathol Rehabil 3(1):1–9
8. BS En 12615 (1999) Products and systems for the protection and repair of concrete structures—test methods—determination of slant shear strength. British Standards Institution, London
9. Courard L, Bissonnette B, Garbacz A, Vaysburd A, Von Fay K, Moczulski G, Morency M (2015) Effect of misalignment on pulloff test results: numerical and experimental assessments. ACI Mater J 112(1):175
10. Decter MH, Keeley C (1997) Durable concrete repair—importance of compatibility and low shrinkage. Constr Build Mater 11(5–6):267–273
11. Diab AM, Abd Elmoaty AEM, Tag Eldin MR (2017) Slant shear bond strength between self compacting concrete and old concrete. Constr Build Mater 130:73–82
12. Emmons PH, Vaysburd AM, McDonald JE (1993) A rational approach to durable concrete repairs. Concr Int 15(9):40–45
13. IS:455 (2005) Indian Standard Portland Slag Cement— Specification. Bureau of Indian Standards, New Delhi, May 1990
14. IS 12269 (2013) Indian Standard Ordinary Portland Cement, 53 Grade—Specification. Bureau of Indian Standards, New Delhi
15. IS 1489 (1991) Indian Standard Portland–Pozzolana Cement—Specification. Bureau of Indian Standards, New Delhi, India
16. IS 456 (2000) Indian Standard Plain and Reinforced Concrete—Code of Practice. Bureau of Indian Standards, New Delhi
17. Júlio ENBS, Branco FAB, Silva VD (2004) Concrete-to-concrete bond strength. Influence of the roughness of the substrate surface. Constr Build Mater 18(9):675–681
18. Kreigh J (1976) Arizona slant shear test: a method to determine epoxy bond strength. ACI J 73(7):372–373
19. Momayez A, Ehsani MR, Ramezanianpour AA, Rajaie H (2005) Comparison of methods for evaluating bond strength between concrete substrate and repair materials. Cem Concr Res 35(4):748–757
20. Naderi M (2009) Analysis of the slant shear test. J Adhes Sci Technol 23(2):229–245
21. Nayak D, Pattnaik RR, Bhoi KC, Panda BC (2019) Investigation into material strength and direction of applied forces to assess bonding behaviour of micro-concrete. J Inst Eng (India) Ser A 100(1):75–82
22. Pattnaik RR (2017) Investigation on failures of composite beam and substrate concrete due to drying shrinkage property of repair materials. J Inst Eng (India) Ser A 98(1–2):85–93

23. Pattnaik RR, Rangarajru PR (2014) Relationship between properties and compatibility of repair materials with substrate concrete. Indian Concr J 88(12):20–31

24. Pattnaik RR, Rangaraju PR (2007) Analysis of compatibility between repair material and substrate concrete using simple beam with third point loading. J Mater Civ Eng 19(12):1060–1069

25. Piancastelli EM, Magalhães AG, Silva FJ, Rezende MAP, Santos WJ, Carrasco EVM, Mantilla JNR (2017) Bond strength between old and new concretes with focus on the strengthening of reinforced concrete columns-slant shear test versus double sleeve test. Appl Mech Mater 864:324–329

26. Poston RW, Kesner K, McDonald JE, Vaysburd AM, Emmons PH (2001) Concrete repair material performance—laboratory study. ACI Mater J 98(2):137–147

27. Saldanha R, Júlio E, Dias-Da-Costa D, Santos P (2013) A modified slant shear test designed to enforce adhesive failure. Constr Build Mater 41:673–680

28. Santos PMD, Julio ENBS (2011) Factors affecting bond between new and old concrete. ACI Mater J 108(4):449–456

29. Vaysburd A, Emmons P, Mailvaganam N, McDonald J, Bissonnette B (2004) Concrete repair technology: a revised approach is needed. Concr Int 26(1):58–65

30. Wall JS, Shrive NG (1988) Factors affecting bond between new and old concrete-fem.pdf. ACI Mater J 85(2):117–125